

Journal of Materials Chemistry A

Accepted Manuscript



This is an *Accepted Manuscript*, which has been through the Royal Society of Chemistry peer review process and has been accepted for publication.

Accepted Manuscripts are published online shortly after acceptance, before technical editing, formatting and proof reading. Using this free service, authors can make their results available to the community, in citable form, before we publish the edited article. We will replace this *Accepted Manuscript* with the edited and formatted *Advance Article* as soon as it is available.

You can find more information about *Accepted Manuscripts* in the [Information for Authors](#).

Please note that technical editing may introduce minor changes to the text and/or graphics, which may alter content. The journal's standard [Terms & Conditions](#) and the [Ethical guidelines](#) still apply. In no event shall the Royal Society of Chemistry be held responsible for any errors or omissions in this *Accepted Manuscript* or any consequences arising from the use of any information it contains.

High-Performance Metal-Free Hydrogen-Evolution Reaction Electrocatalyst from Bacteria Derived Carbon

Cite this: DOI: 10.1039/x0xx00000x

Received 00th January 2015,
Accepted 00th January 2015

DOI: 10.1039/x0xx00000x

www.rsc.org/

Li Wei,^a Huseyin Enis Karahan,^a Kunli Goh,^a Wenchao Jiang,^a Dingshan Yu,^a Özgür Birer,^{b,c} Rongrong Jiang and Yuan Chen^{a*}

We report a sustainable approach to obtain carbon materials with nitrogen and phosphor dual functionalities from a common bacterium strain (*S. aureus*) as a highly efficient hydrogen-evolution reaction (HER) catalyst. With mesoporous structure introduced by ZnCl₂ salt and cathodic activation, it demonstrates an onset overpotential as low as 76 mV, Tafel slope of 58.4 mV/dec and large normalized exchange currently density at 1.72×10⁻² mA/cm², which is comparable to hitherto best metal-free and well-fabricated metallic HER catalysts.

Using renewable energy sources generated electrical energy to reduce water through hydrogen-evolution reaction (HER) is a sustainable route of producing hydrogen as an energy carrier.^{1, 2} Platinum (Pt) based catalysts have efficient catalytic performances for HER; however their applications are hampered by high cost and insufficient Pt reserves.³⁻⁵ Substantial efforts have been devoted to developing electrocatalysts based on non-noble metals (Fe, Co, Ni, Mo), including transition-metal chalcogenides, nitrogen or phosphorus metal derivatives, carbides, metal complex and alloys; despite the fact that they often suffer from corrosion in acidic electrolytes.⁶⁻¹⁸ Carbon materials have long been used as supports for HER catalysts.¹⁹⁻²² Recent efforts in forming strongly coupled inorganic/carbon hybrid materials as HER catalysts have shown improved activity and durability.²³ Furthermore, several studies demonstrated carbon materials, such as graphene, carbon nanotubes, carbon nitride, and their hybrids, can work as efficient metal-free HER catalysts.²⁴⁻³⁰ The synthesis of HER catalysts usually requires high purity chemicals and gases, excessive amount of strong acids and bases, or costly organic precursors. Thus, it is desirable to develop innovative green and sustainable methods to obtain high-performance HER catalysts.

Herein, we demonstrate that carbon material derived from a common bacterium strain (*Staphylococcus aureus* (*S. aureus*, ATCC 6538)) is a high-performance metal-free HER catalyst. There are

several advantages of using bacteria to obtain carbon materials as HER catalysts: (1) as living organisms, bacteria are comprised mainly of C, H, O, N, P, S and trace amount of other elements. Their rich N and P contents provide abundant heteroatoms to dope carbon materials,³¹ which could serve as catalytic active sites for HER. (2) Bacterial cells have a variety of highly porous cellular structures, which can lead to a large surface area and potentially controllable pore structures in carbon materials.³² (3) The industrial fermentation process has the capability of producing bacteria cost-effectively in large quantity for scalable catalyst production.³³ (4) The fast developing biotechnology provides many tools to genetically modify bacteria and enrich them with specific elements, which can lead to carbon materials with tailored heteroatom functionalities.

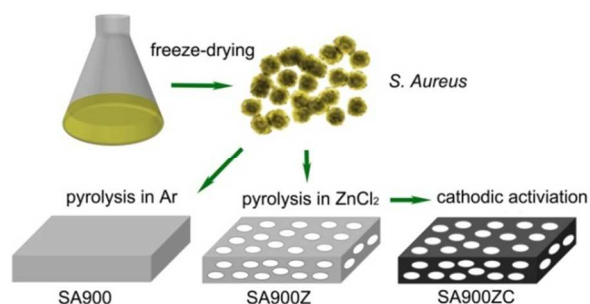


Fig 1. An illustration of the synthetic procedure for HER carbon catalysts derived from *S. aureus*.

As illustrated in Fig 1, *S. aureus* cells were first cultivated in lysogeny broth (LB) media at 37 °C for 10 h. The cultivated cells are spherical in shape with an average diameter of ~0.5 μm. (Fig 2a). The freeze-dried cells were first directly carbonized in Ar flow (100 sccm) at 900 °C for 3 h to yield the first carbon material denoted as SA900. HER on carbon catalysts is a surface reaction which would be more efficient on catalysts with a large surface area.³⁴ A Lewis

acid (ZnCl_2) has been used to generate mesopores in carbon materials.³⁵ Here, we mixed freeze-dried cells with ZnCl_2 at the weight ratio of 1:4, and then carbonized the mixture in Ar flow at 900 °C for 3 h to yield the second carbon material denoted as SA900Z. Cathodic treatment is an effective method to activate solid electrode materials.^{36, 37} This method has recently been applied to carbon nanotubes to increase their catalytic activity for HER.^{26, 27} In this work, SA900Z underwent a 4-h cathodic treatment at -2 V vs. saturated calomel electrode (SCE) to yield the third carbon material, denoted as SA900ZC. Furthermore, two additional carbon catalysts, thermally reduced graphene oxide (rGO) and N-doped graphene (NG) were also prepared as references (see ESI for detailed experimental procedures).

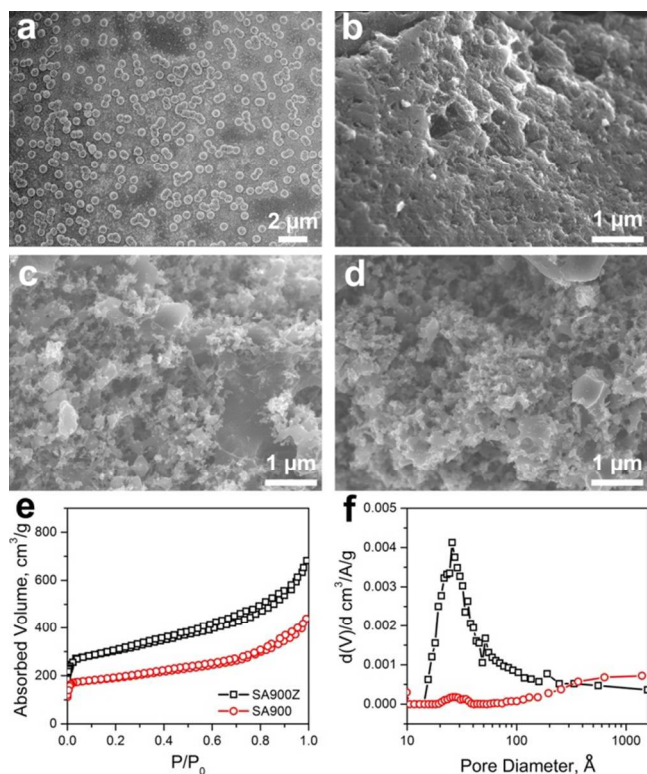


Fig 2. Physical properties of *S. aureus* derived carbon materials. SEM images of (a) freeze-dried *S. aureus* cells, (b) SA900, (c) SA900Z, and (d) SA900ZC. (e) N_2 physisorption isotherms and (f) pore size distribution of SA900 and SA900Z.

Morphology of bacterium derived carbon materials was first investigated by field emission scanning electron microscope (FE-SEM). Fig 2b shows that SA900 has many pores larger than 100 nm. In contrast, SA900Z (Fig 2c) has a larger number of smaller pores. Fig 2e indicates that the specific surface area of SA900 and SA900Z by the Brunauer–Emmett–Teller method is 341 and 816 m^2/g , respectively. Their Barrett–Joyner–Halenda pore size distribution (Fig 2f) confirms that SA900 have larger pores, while SA900Z contains many mesopores at the diameter centred ~3 nm. The SEM image (Fig 2d) displays no significant differences between SA900Z and SA900ZC, suggesting that the cathodic treatment did not induce major structural changes.

The physicochemical properties of the carbon materials were further characterized by spectroscopies. Raman spectra (Fig 3a) show G-band peaks at $\sim 1590 \text{ cm}^{-1}$, demonstrating the successful formation of graphitic carbon. The intensity of D-band peak at $\sim 1320 \text{ cm}^{-1}$ increases in SA900Z and SA900ZC in accordance with the addition of mesopores, which exposes more edges enriched with non-hexagonal carbon defects. X-ray photoelectron spectroscopy (XPS) analysis found that the freeze-dried cells contain 70.4 at% C, 7.1 at% O, 14.9 at% N, 7.1 at% P, 5.4 at% S, 0.8 at% Si and other trace amount of elements, such as Na, K and Ca. A typical XPS survey spectrum of SA900 is presented in Fig 3b. C, O, N and P were identified as the four major elements. Being compared to the dried cells, the abundances of O, N and P decrease after carbonization. They distribute uniformly throughout the carbon material as confirmed by EDX element mapping (Fig 3d-g). Physicochemical properties and element compositions of all carbon materials studied in this work are listed in Table S1 for comparison. The abundances of N and P decrease slightly after mesopore addition, while the cathodic treatment further reduces N and P abundances while increases O abundance. It should be pointed out that the abundance of N and P can be further regulated to some extent by cell culturing conditions. In this work, a native *S. aureus* strain was used. It is feasible to use bioengineering tools to produce engineered bacteria enriched with higher concentrations of N and P.

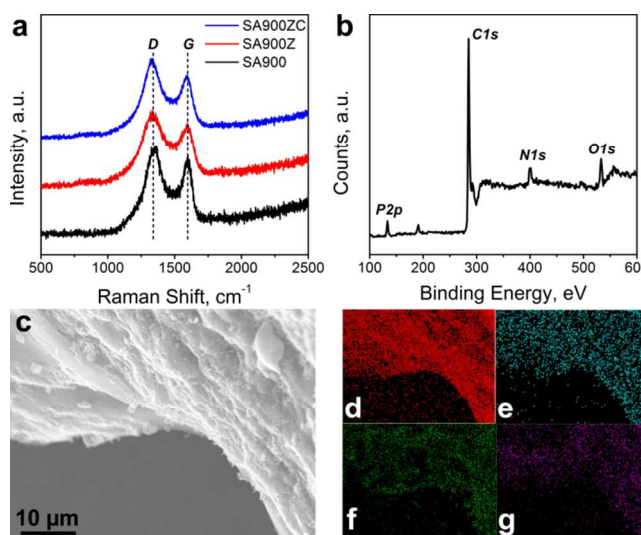


Fig 3. Chemical properties of *S. aureus* derived carbon materials. (a) Raman spectra, (b) XPS spectrum of SA900Z, (c) SEM image of SA900, (d-f) with the corresponding EDX maps of C, O, N and P.

The HER catalytic performances of the bacterium derived carbon catalysts were examined by cyclic voltammetry together with rGO and NG as reference catalysts. Fig 4a displays their linear sweep voltammetry (LSV) polarization curves in a N_2 saturated 0.5 M H_2SO_4 electrolyte in the three-electrode configuration at the scan rate of 2 mV/s. The carbon catalysts on every working electrode have a mass loading of $\sim 0.03 \text{ mg}$, *i.e.* a mass density of $\sim 0.152 \text{ mg}/\text{cm}^2$ deposited on glassy carbon (GC) electrodes. Their preparation procedure is detailed in the Supporting Information. The HER activity is evaluated from two aspects. First, we compared their onset overpotential, defined as the overpotential (η) to achieve

the current density (j) of 0.25 mA/cm^2 . rGO has a very high onset overpotential close to that of the GC electrode without carbon catalysts, suggesting that rGO has negligible HER activity. For NG, η drops to 316 mV (vs. reversible hydrogen electrode, RHE), confirming that N doping can improve the HER activity of graphene-based materials. The onset overpotentials of SA900 and SA900Z further decrease to 254 and 236 mV, respectively, which are similar to that of N and P dual-doped graphene materials reported in the literature.²⁴ The onset overpotential of SA900ZC further drops to 76 mV, approaching hitherto the best value obtained on single walled carbon nanotube (SWCNT) electrodes after very long cathodic treatments (144 h).²⁷ In fact, SA900ZC has one of the lowest onset overpotential among metal-free HER catalysts reported so far (Table S2). Second, we examined the η required to achieve j of 10 mA/cm^2 , which is another commonly used criterion to evaluate the performance of HER catalysts.^{24, 29, 38} It is 506 mV for NG, 419 mV for SA900, 387 mV for SA900Z and 204 mV for SA900ZC. The performances of SA900 and SA900Z are comparable to that of the N and P dual-doped graphene materials.²⁴ SA900ZC is close to that of the 144 h-activated SWCNTs (Table S2).²⁷

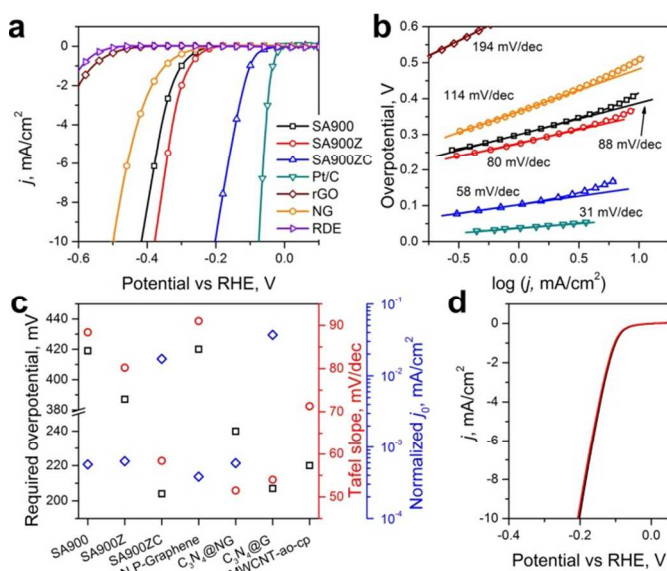


Fig 4. (a) HER LSV polarization curves and (b) corresponding Tafel plots of *S. Aureus* derived carbon catalysts together with rGO and NG references at the scan rate of 2 mV/s in 0.5 M H_2SO_4 . (c) Performance comparison between *S. aureus* derived carbon catalysts and recently reported metal-free HER catalysts^{24-26, 29} in terms of the potential required to achieve the current density of 10 mA/cm^2 (\square), Tafel slope (\circ), and normalized exchange current density (\diamond). (d) LSV curves of SA900ZC before and after 5000 CV cycles.

Next, HER activity of these carbon catalysts was further examined through their Tafel plots (Fig 4b). As a typical surface reaction, the pathway of HER has several steps, which is initialized by the adsorption of H^+ (Volmer step) and followed by either Heyrovsky step (electrochemical desorption) or Tafel step (chemical desorption) to generate and release H_2 .³⁹ The Tafel slope of rGO and NG calculated from the linear part of their Tafel plots is 194 and 114 mV/dec, respectively, which suggests that the initial H^+ adsorption is the rate limiting step (slope $> 120 \text{ mV/dec}$). In contrast, the Tafel slope of SA900 and SA900Z drops to 88 and 80 mV/dec, respectively, suggesting a transition of the rate limiting step from the

Volmer step to the Heyrovsky step (slope between 40 to 120 mV/dec).³⁹ The Tafel slope of SA900ZC further decreases to 58.4 mV/dec, indicating a much reduced energy barrier for the electrochemical desorption of H_2 . The exchange current density (j_0) of SA900 and SA900Z was also derived from their Tafel plots. SA900Z has higher j_0 ($0.54 \times 10^{-3} \text{ mA/cm}^2$) over SA900 ($0.32 \times 10^{-3} \text{ mA/cm}^2$). The j_0 of SA900ZC greatly increases to $17.23 \times 10^{-3} \text{ mA/cm}^2$, which is one of the highest reported for metal-free HER catalysts (Table S3). In order to normalize the measured j_0 for easy comparison with other literature data, we estimated the electrochemically active surface area of carbon catalysts by assessing their electrochemical double layer capacitance (C_{dl}) using a cyclic voltammetry method (see ESI for detailed experimental procedure) (Fig S1). The measured C_{dl} and normalized j_0 by mass were given in Table S3 together with recently reported carbon or non-noble metal HER catalysts. As showed in Fig 4c, the normalized j_0 of SA900 and SA900Z is 0.567×10^{-3} and $0.629 \times 10^{-3} \text{ mA/cm}^2$, respectively, which is comparable to that of N,P-graphene²⁴ and $\text{C}_3\text{N}_4@\text{NG}$.³⁸ SA900ZC has much higher normalized j_0 at $1.72 \times 10^{-2} \text{ mA/cm}^2$, approaching that of $\text{C}_3\text{N}_4@\text{G}$.²⁹ Furthermore, SA900ZC also has good durability. Fig 4d shows that minor performance changes after 5000 cycles of CV scan from 0 to -0.8 V (vs RHE).

The origin of the high HER activity from the bacterium derived carbon catalysts was explored by XPS analysis. The high resolution XPS spectra of C, O, N and P in SA900, SA900Z, and SA900ZC are presented in Fig S3. Their deconvoluted elemental compositions and heteroatom banding status are listed in Table S4. Comparing SA900 with rGO and NG, the latter has a larger surface area and more abundant pore structures (Fig S2). Their electrical conductivity (measured by electrochemical impedance spectroscopy (Fig S4) is similar. NG contained an even higher concentration of doped N (Table S1). The key difference among them is that SA900 has a 4.23 at% of doped P. A recent study has shown a negative Gibbs free-energy for hydrogen adsorption in N, P-dual doped graphene structures.²⁴ The synergistic effects of N and P in graphene-based materials could significantly increase their HER activity.²⁴ SA900 contains both N and P, resulting from the bacterium cells. Thus, we propose that better HER activity of SA900 compared to NG could also come from the synergistic effects of N and P. N and P contents drop slightly in SA900Z after introducing mesopores. There are some minor changes in the heteroatom bonding states between SA900 and SA900Z (Table S4). After introducing mesopores, the BET surface area of SA900Z is 2.39 times of that of SA900. However, electrochemically active surface area, estimated by C_{dl} (Table S3) of SA900Z is only 1.54 times of that of SA900. The value of j_0 of SA900Z, which directly correlates with the catalytically active sites, is 1.69 times of that of SA900. The change in j_0 is comparable to the change in the effective electrochemical surface area, which implies that some surface area of SA900Z which is assessable to liquid N_2 still cannot be accessed by electrolytes.

The most significant increase in HER activity was observed in SA900ZC after the cathodic treatment. Cathodic treatment can change the surface microstructure and chemistry of electrodes.³⁶ It has been found that cathodic treatment of graphite in an acidic electrolyte would cleave the graphite basal plane to form active edges with more oxygen containing functional groups.⁴⁰ Enhanced HER performance induced by cathodic treatment could be attributed to oxygenated functional groups, which may serve as H^+ acceptor or

proton relays to facilitate the H₂ formation. Similar mechanism was proposed to explain the HER activity of a metal-centered hydrogenase, C₆₀(OH)₈ and activated carbon nanotubes.^{26, 28, 41} In this work, we observed that the D-band to G-band ratio of Raman spectra increases from 1.064 (SA900Z) to 1.142 (SA900ZC), indicating the formation of defective carbon structures caused by the cathodic treatment. The deconvolution of high resolution XPS spectra of C, N, P and O elements (FigS3 and Table S4) showed that the abundances of oxidized-N, O=C-OR, NO_x, and P-O increase significantly after cathodic treatment despite that the overall contents of both N and P decline. These observations support that the additional oxygenated functional groups induced by the cathodic treatment are responsible for the high performance of SA900ZC.

Conclusions

High performance metal-free hydrogen-evolution reaction catalysts were obtained by carbonizing a common bacterium (*S. aureus*). The bacterium derived carbon materials have a large surface area of 341 m²/g with N and P dual functionalities of 4.88 at% N and 4.23 at% P. Mesopores were further introduced by carbonization together with ZnCl₂ to increase the surface area to 816 m²/g. After a cathodic treatment, the *S. aureus* derived carbon catalyst exhibits highly efficient electrocatalytic activity for HER in acidic electrolyte. It demonstrates a low onset overpotential of 76 mV, Tafel slope of 58.4 mV/dec and large normalized exchange current density at 1.72×10⁻² mA/cm², which is comparable to or even better than that of existing metal-free and well-fabricated metallic catalysts. Excellent activity can be attributed to the synergistic effects of N and P, abundant mesopores, and structural and surface chemistry changes induced by the cathodic treatment. Our work demonstrates the great potential of using bacteria to obtain carbon materials with tailored structure and composition as electrocatalysts for sustainable chemical processes.

Notes and references

^a School of Chemical and Biomedical Engineering, Nanyang Technological University, Singapore 637459. Tel.: +65 63168939. E-mail: chenyan@ntu.edu.sg (Yuan Chen)

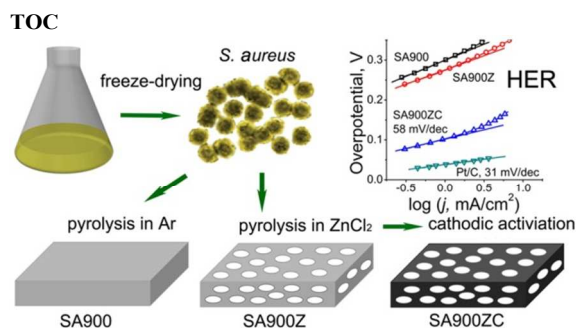
^b Chemistry Department, Koç University, Rumelifeneri Yolu, Sariyer, 34450, Istanbul, Turkey

^c KUYTAM Surface Science and Technology Center, Koç University, Rumelifeneri Yolu, Sariyer, 34450, Istanbul, Turkey

† Electronic Supplementary Information (ESI) available: [details of any supplementary information available should be included here]. See DOI: 10.1039/c000000x/

- J. O. M. Bockris and E. C. Potter, *J. Electrochem. Soc.*, 1952, **99**, 169-186.
- M. G. Walter, E. L. Warren, J. R. McKone, S. W. Boettcher, Q. Mi, E. A. Santori and N. S. Lewis, *Chem. Rev.*, 2010, **110**, 6446-6473.
- N. M. Markovic, B. N. Grgur and P. N. Ross, *J. Phys. Chem. B*, 1997, **101**, 5405-5413.
- N. Toshima, T. Yonezawa and K. Kushihashi, *J. Chem. Soc., Faraday Trans.*, 1993, **89**, 2537-2543.
- Y. Zheng, Y. Jiao, M. Jaroniec and S. Z. Qiao, *Angew. Chem. Int. Ed.*, 2015, **54**, 52-65.
- B. E. Conway and L. Bai, *J. Electroanal. Chem.*, 1986, **198**, 149-175.
- A. Belanger and A. K. Vijh, *J. Electrochem. Soc.*, 1974, **121**, 225-230.
- B. Cao, G. M. Veith, J. C. Neufeind, R. R. Adzic and P. G. Khalifah, *J. Am. Chem. Soc.*, 2013, **135**, 19186-19192.
- R. Bashyam and P. Zelenay, *Nature*, 2006, **443**, 63-66.
- W.-F. Chen, K. Sasaki, C. Ma, A. I. Frenkel, N. Marinkovic, J. T. Muckerman, Y. Zhu and R. R. Adzic, *Angew. Chem. Int. Ed.*, 2012, **51**, 6131-6135.
- R. K. Shervedani and A. Lasia, *J. Electrochem. Soc.*, 1997, **144**, 511-519.
- M. S. Faber, R. Dziedzic, M. A. Lukowski, N. S. Kaiser, Q. Ding and S. Jin, *J. Am. Chem. Soc.*, 2014, **136**, 10053-10061.
- Y. G. Li, H. L. Wang, L. M. Xie, Y. Y. Liang, G. S. Hong and H. J. Dai, *J. Am. Chem. Soc.*, 2011, **133**, 7296-7299.
- M. A. Lukowski, A. S. Daniel, F. Meng, A. Forticaux, L. S. Li and S. Jin, *J. Am. Chem. Soc.*, 2013, **135**, 10274-10277.
- E. J. Popczun, J. R. McKone, C. G. Read, A. J. Biacchi, A. M. Wilttrout, N. S. Lewis and R. E. Schaak, *J. Am. Chem. Soc.*, 2013, **135**, 9267-9270.
- Y. J. Sun, C. Liu, D. C. Grauer, J. K. Yano, J. R. Long, P. D. Yang and C. J. Chang, *J. Am. Chem. Soc.*, 2013, **135**, 17699-17702.
- J. F. Xie, J. J. Zhang, S. Li, F. Grote, X. D. Zhang, H. Zhang, R. X. Wang, Y. Lei, B. C. Pan and Y. Xie, *J. Am. Chem. Soc.*, 2013, **135**, 17881-17888.
- J. R. McKone, S. C. Marinescu, B. S. Brunschwig, J. R. Winkler and H. B. Gray, *Chem. Sci.*, 2014, **5**, 865-878.
- S. A. Grigoriev, P. Millet and V. N. Fateev, *J. Power Sources*, 2008, **177**, 281-285.
- S. H. Joo, S. J. Choi, I. Oh, J. Kwak, Z. Liu, O. Terasaki and R. Ryoo, *Nature*, 2001, **412**, 169-172.
- S. Yin, Y. Goldovsky, M. Herzberg, L. Liu, H. Sun, Y. Zhang, F. Meng, X. Cao, D. D. Sun, H. Chen, A. Kushmaro and X. Chen, *Adv. Funct. Mater.*, 2013, **23**, 2972-2978.
- Y. Li, H. Wang, L. Xie, Y. Liang, G. Hong and H. Dai, *J. Am. Chem. Soc.*, 2011, **133**, 7296-7299.
- Y. Y. Liang, Y. G. Li, H. L. Wang and H. J. Dai, *J. Am. Chem. Soc.*, 2013, **135**, 2013-2036.
- Y. Zheng, Y. Jiao, L. H. Li, T. Xing, Y. Chen, M. Jaroniec and S. Z. Qiao, *ACS Nano*, 2014, **8**, 5290-5296.
- Y. Zheng, Y. Jiao, Y. Zhu, L. H. Li, Y. Han, Y. Chen, A. Du, M. Jaroniec and S. Z. Qiao, *Nature Commun.*, 2014, **5**.
- W. Cui, Q. Liu, N. Cheng, A. M. Asiri and X. Sun, *Chem. Commun.*, 2014, **50**, 9340-9342.
- R. K. Das, Y. Wang, S. V. Vasilyeva, E. Donoghue, I. Pucher, G. Kamenov, H.-P. Cheng and A. G. Rinzler, *ACS Nano*, 2014, **8**, 8447-8456.
- J. Zhuo, T. Wang, G. Zhang, L. Liu, L. Gan and M. Li, *Angew. Chem. Int. Ed.*, 2013, **52**, 10867-10870.
- Y. Zhao, F. Zhao, X. Wang, C. Xu, Z. Zhang, G. Shi and L. Qu, *Angew. Chem. Int. Ed.*, 2014, 13934-13939.
- K. Xie, H. Wu, Y. Meng, K. Lu, Z. Wei and Z. Zhang, *J. Mater. Chem. A*, 2015, **3**, 78-82.

31. M. Heldal, S. Norland and O. Tumyr, *Appl. Environ. Microbiol.*, 1985, **50**, 1251-1257.
32. T. Klaus-Joerger, R. Joerger, E. Olsson and C.-G. Granqvist, *Trends Biotechnol.*, 2001, **19**, 15-20.
33. E. Russo, *Nature*, 2003, **421**, 456-457.
34. W. Sheng, H. A. Gasteiger and Y. Shao-Horn, *J. Electrochem. Soc.*, 2010, **157**, B1529-B1536.
35. P. Kuhn, A. Forget, D. Su, A. Thomas and M. Antonietti, *J. Am. Chem. Soc.*, 2008, **130**, 13333-13337.
36. G. M. Swain, in *Handbook of Electrochemistry*, ed. C. G. Zoski, Elsevier, Amsterdam, 2007, pp. 111-V.
37. S. Trasatti, in *Advances in Electrochemical Science and Engineering*, Wiley-VCH Verlag GmbH, 2008, pp. 1-85.
38. Y. Zheng, Y. Jiao, Y. Zhu, L. H. Li, Y. Han, Y. Chen, A. Du, M. Jaroniec and S. Z. Qiao, *Nat Commun*, 2014, **5**, 3783.
39. B. E. Conway and B. V. Tilak, *Electrochim. Acta*, 2002, **47**, 3571-3594.
40. T. Shimada, S. Kubota, T. Yanase and T. Nagahama, *Carbon*, 2014, **67**, 300-303.
41. Y. Nicolet, A. L. de Lacey, X. Vernède, V. M. Fernandez, E. C. Hatchikian and J. C. Fontecilla-Camps, *J. Am. Chem. Soc.*, 2001, **123**, 1596-1601.



One sentence:

Nitrogen and phosphor dually doped mesoporous carbon derived from bacteria as high performance electrocatalyst for hydrogen evolution reaction.